

Directional 3D Real-time Dual-polarized Measurement of Wideband Mobile Radio Channel

Kimmo Kalliola^{1,2}, Heikki Laitinen³, Leo Vaskelainen³, and Pertti Vainikainen¹

¹ Helsinki University of Technology, Radio Laboratory, P.O.Box 3000, FIN-02015 HUT, Finland

² Nokia Research Center, P.O.Box 407, FIN-00045 Nokia Group, Finland

³ VTT Information Technology, Telecommunications, P.O.Box 1202, FIN-02044 VTT, Finland

Abstract

The measurement method presented in this paper enables the complete characterization of the mobile radio channel including polarization, Doppler behavior, and three-dimensional spatial information (azimuth, elevation, and delay) of the signal multipath components. The method is based on a wideband radio channel sounder and a spherical antenna array. The measurement method enables the separation of multipaths with the same excess delay and Doppler shift as long as their angular separation is not less than 40°, and path loss difference not larger than 10 dB. The polarization vector of the signal can also be measured with 9 dB dynamic range. The achieved delay resolution is 33 ns, which corresponds to path length of 10 m. The maximum mobile speed for ±2 % phase accuracy is 10 m/s. The measured channel statistics can be used for evaluation of antennas for mobile handsets, as well as developing polarization and radiation pattern diversity antennas for handsets.

1. Introduction

The demand for higher data rates sets high requirements for the future wireless communication systems. Efficient use of limited frequency spectrum requires thorough understanding of the behavior of the system, including the radio channel, which is the most difficult part to model. This understanding can be obtained either by prediction based on e.g. ray tracing simulations, or measurements of real channels. The former approach requires reliable simulation tools that, themselves, must be verified with measurement data.

The radio channel is a complex function of time, frequency, space, direction, and polarization. Therefore the directional real-time measurement of the channel is not an

easy task. It requires simultaneous (or nearly simultaneous) reception of the same signal from multiple antenna elements, i.e. the elements of an antenna array. The direction-of-arrival (DOA) of the signal can be estimated based on the phase differences between the elements of the array. So far the reported real-time directional channel measurements have been limited to two dimensions, i.e. the delay and azimuth angle of the signal [1,2]. This kind of measurement typically aims to describe the directional signal environment seen from a base station (BS) of a cellular system. Typically the elevation angle of different incoming signals or multipath components of one signal does not vary significantly at the BS. At the mobile end of the channel, however, the situation can be totally different. For example inside buildings or in street canyons the scatterers close to the mobile cause signal spreading in all three dimensions. The complexity of the realistic environments makes this very difficult to model, and the statistics of the phenomenon are still mostly unknown.

This paper presents a method for directional three-dimensional real-time measurements of the wideband mobile radio channel. It enables the complete characterization of the mobile radio channel including the delay, polarization, Doppler shift, and direction of the signal multipath components. The method is based on a wideband radio channel sounder and a spherical antenna array to collect the directional information in three dimensions.

The measured channel statistics can be used for evaluation of antennas for mobile handsets, as well as for developing polarization and radiation pattern diversity antennas for handsets.

In this paper the measurement system is described, and different approaches to determine the directional channel information presented. The directional properties of the array are defined with test measurements.

2. Description of measurement system

The measurement system is based on a spherical array of 32 dual-polarized antenna elements and a complex wideband radio channel sounder [3]. A wideband signal is transmitted using a fixed antenna, and received separately with each of the 32 elements and both polarizations, using a fast RF switch. The carrier frequency of the sounder is 2.154 GHz, and the chip frequency of the modulating pseudo-random sequence in the transmitter can be selected up to 30 MHz, resulting in delay resolution of 33 ns. The received demodulated signal is divided into I- and Q- branches and sampled with two 120 Ms/s A/D-converters. The signal samples from each branch of the switch are then stored for-off line processing to obtain the complex impulse response (IR) of the channel corresponding to each element and polarization. The number of switched branches is 64, which gives a maximum of 32 antenna elements with separate feeds for θ - and ϕ -polarizations. The switching is very fast: one impulse response with e.g. 4 μ s delay window is measured from every element in 64.4 μ s = 256 μ s. At normal mobile speeds the channel can be assumed static over this period. For example at 10 m/s the maximum phase error between the array elements is ± 2 % at 2.154 GHz. Thus, real-time measurements can be made.

2.1 Array geometry

The ideal way to cover the whole 4π angle in space with direction-independent angular resolution would be to use equally spaced elements on the surface of a sphere. However, it is not possible to distribute any number of points on a sphere with each one equidistant from its neighbors. In other words, regular polyhedra exists only for certain numbers of vertices, and 32 is not one of them.

The geometry of the built array is based on the dual of the Archimedian solid, the truncated icosahedron, which is probably best known today as the geometry of the football. In this configuration, two different distances between adjacent elements exist. The nearest neighbors of an element are always at a distance of $0.641R$ and the next at $0.714R$ from the element, where R is the radius of the sphere. Each element has either five or six such neighbors. It is shown in [4] that this arrangement minimizes the Coulombic potential of a system of 32 point charges distributed on the surface of a sphere, thus approximating an even distribution.

To reduce cabling and losses, the element switching unit is placed inside the spherical array. Only one signal cable and two control cables are lead out from the array, which minimizes the disturbance to the near field of the array. The radius of the built array is $R = 170$ mm (1.22λ

at 2.154 GHz). A smaller radius would result in lower sidelobe level (directional dynamics), but the physical size of the switching unit limits the practically achieved radius.

2.2. Array element

The main requirements for the element of the array are two independent orthogonal polarizations with high cross-polarization discrimination, and sufficient bandwidth to meet the requirement of the measurement system. Directive element is also desirable for the spherical array. The geometry of the array element is presented in Figure 1.

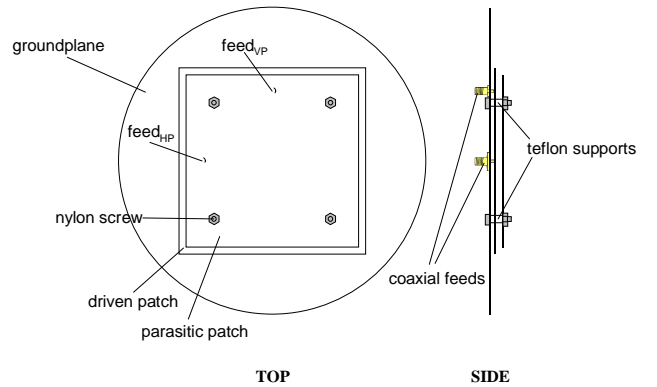


Figure 1. Geometry of the element of the spherical array.

The 6-dB beamwidth of the element is 90° in the E-plane and 100° in the H-plane. The polarization discrimination is better than 18 dB within 6-dB beamwidth. The measured gain of the element is 7.8 dB. The return loss is over 10 dB inside the whole measurement band (2154 \pm 30 MHz).

2.3. Built array

The antenna elements are mounted on a spherical surface consisting of two hollow aluminum hemispheres with outer diameter of 330 mm. The elements are isolated from the mount, and the distance from the center of the fed patch (see Figure 1) to the center of the sphere is 170 mm. The elements point towards the normal of the sphere and they are oriented so that the polarization vectors corresponding to the feeds are parallel to unit vectors \mathbf{u}_θ and \mathbf{u}_ϕ . The 64-channel RF switching unit is placed inside the ball together with its control electronics. Only the RF signal cable, two coaxial control cables, and the power supply wires are lead outside the ball. Figures 2 and 3 present the configuration of the spherical array and the switching unit placed inside it.



Figure 2. Spherical array of 32 dual-polarized microstrip patch elements.

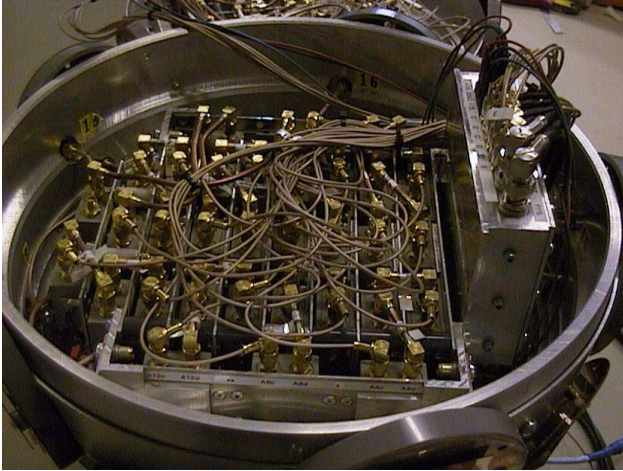


Figure 3. Lower hemisphere of spherical array. Switching unit placed inside the array can be seen.

3. Direction finding with spherical array

The far field of an arbitrary group of N dual-polarized antenna elements at direction (θ, ϕ) can be expressed as:

$$\mathbf{E}(\theta, \phi) = q \sum_{n=1}^N w_n e^{j \frac{2\pi}{\lambda} \mathbf{r}_n \cdot \mathbf{u}(\theta, \phi)} [h_n \mathbf{g}_n^H(\theta, \phi) + v_n \mathbf{g}_n^V(\theta, \phi)] \quad (1)$$

where:

- q = array input signal
- w_n = complex weight of element n
- \mathbf{r}_n = position vector of element n
- $\mathbf{u}(\theta, \phi)$ = unit vector pointing at direction (θ, ϕ)
- $\mathbf{g}_n(\theta, \phi)$ = field pattern of element n

Superscripts H and V denote the local horizontal and vertical polarization vectors of the antenna elements (oriented parallel to \mathbf{u}_ϕ and \mathbf{u}_θ), respectively. Coefficients h_n and v_n are applied to take into account the location-dependent orientation of the element polarization vectors, and are defined as:

$$\begin{aligned} h_n &= \mathbf{p} \cdot \mathbf{u}_\phi(\theta_n, \phi_n) \\ v_n &= \mathbf{p} \cdot \mathbf{u}_\theta(\theta_n, \phi_n) \end{aligned} \quad (2)$$

where \mathbf{p} is the desired polarization vector, for which the field is to be calculated (typically horizontal or vertical).

The complex weight vector w can be used to form a beam towards a desired direction. The 3D angular response of the radio channel can be measured by forming a grid of beams covering the whole 4π solid angle. Two methods to determine the corresponding weight vectors are presented in the following.

3.1. Beamforming

The simplest method to create a beam towards a certain direction (θ_0, ϕ_0) is to phase the element signals in that direction. In this case the weights are written as:

$$w_n(\theta_0, \phi_0) = a_n(\theta_0, \phi_0) e^{-j \frac{2\pi}{\lambda} \mathbf{r}_n \cdot \mathbf{u}(\theta_0, \phi_0)} \quad (3)$$

where a_n is an amplitude tapering coefficient to suppress the array sidelobes.

If s_n and t_n are the signals measured from element n at two orthogonal polarizations (H and V), the angular response becomes:

$$S(\theta, \phi) = \sum_{n=1}^N [h_n(\theta, \phi) s_n + v_n(\theta, \phi) t_n] w_n(\theta, \phi), \quad (4)$$

$$\begin{cases} \theta = -90^\circ \dots +90^\circ \\ \phi = -180^\circ \dots +180^\circ \end{cases}$$

Let us assume a single plane wave with amplitude \mathbf{q} arriving at the array from direction (θ_s, ϕ_s) . In this case

signals s_n and t_n contain the direction-dependent phase information corresponding to the location of the element, and they are weighted by the element pattern at (θ_s, ϕ_s) :

$$\begin{bmatrix} s_n \\ t_n \end{bmatrix} = e^{j\frac{2\pi}{\lambda}\mathbf{r}_n \cdot \mathbf{u}(\theta_s, \phi_s)} \begin{bmatrix} \mathbf{g}_n^H(\theta_s, \phi_s) \cdot \mathbf{q} \\ \mathbf{g}_n^V(\theta_s, \phi_s) \cdot \mathbf{q} \end{bmatrix} \quad (5)$$

Substituting this to Eq. (4) and using element phasing from Eq. (3), gives

$$S(\theta, \phi) = \sum_{n=1}^N a_n(\theta, \phi) e^{-j\frac{2\pi}{\lambda}[\mathbf{r}_n \cdot \mathbf{u}(\theta, \phi) - \mathbf{r}_n \cdot \mathbf{u}(\theta_s, \phi_s)]} \cdot [h_n \mathbf{g}_n^H(\theta_s, \phi_s) \cdot \mathbf{q} + v_n \mathbf{g}_n^V(\theta_s, \phi_s) \cdot \mathbf{q}] \quad (6)$$

It can be seen that the maximum of the response is produced towards direction $(\theta = \theta_s, \phi = \phi_s)$. Highest level is produced if the signal polarization vector \mathbf{q} is matched to the desired polarization vector \mathbf{p} . The remaining part of the response is not zeros, but spurious responses whose level depends on the geometry of the array, and the amplitude tapering term a_n . These are equivalent to sidelobes of an antenna array.

The proposed tapering function for spherical array is the normalized power function written as

$$a_n(\theta, \phi) = \left(\frac{R + \mathbf{r}_n \cdot \mathbf{u}(\theta, \phi)}{2R} \right)^p \quad (7)$$

where R is the radius of the sphere. The weight of the element pointing at the desired direction is unity while the element pointing at the opposite direction is nulled.

3.2. Beam synthesis method

In addition to beamforming based on simple phasing, the weight vector corresponding to a beam in certain direction can be found through numeric beam synthesis. In the directional channel measurement approach this method can be applied to suppress the sidelobe level of the array. A suitable method for conformal arrays is the iterative least-squares synthesis presented in [5].

The method is based on minimizing the difference between the radiation pattern and a given target function. To produce a grid of beams for directional scanning, the target function has to be rotated for each discrete angle in the desired grid, as well as for both horizontal and vertical polarization.

In our case of the spherical array the used target function was a beam with 3-dB beamwidth of 33° and sidelobe

level better than -19 dB. The function was computed for 5° angular grid.

4. Array directional properties

In radio channel sounding, the delay dimension of the channel is solved based on the wideband transmitted signal. The angular dimension, on the other hand, can be computed from the relative phases of the impulse responses measured from different array elements.

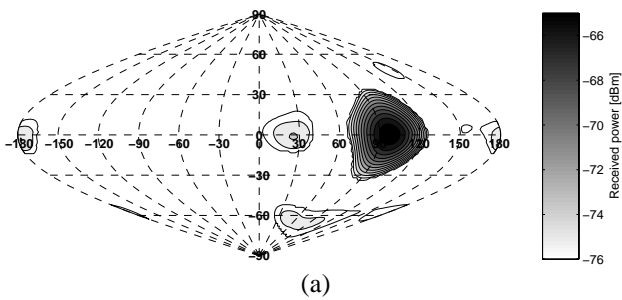
The directional and polarization accuracy of the measured radio channel can be characterized by the angular resolution, directional dynamics, and cross polarization discrimination (XPD), which describe the ability to separate two signals close to each other, with large power difference, or having different polarization vectors. They correspond to the 3 dB beamwidth (Δ_{3dB}), sidelobe level (SLL), and XPD of the array used in the measurement. Each of these parameters depend on the array itself, but also on the used analysis method.

The directional properties of the built array have been studied by measuring the impulse response of a known signal environment, using one and two signal vertically polarized signal sources in an anechoic chamber. The directional responses have been calculated for both the beamforming and beam synthesis methods. In the case of anechoic chamber, the measured impulse response contains only one tap. The directional responses were calculated for the tap only. In measurements of real channels, the calculation will be done for each tap (multipath) separately.

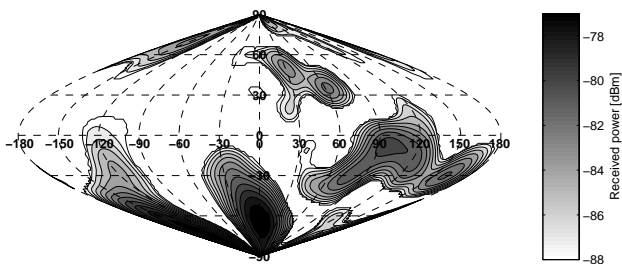
For beamforming method the responses were computed for 2° grid using Eq. (4) with weights given in Eq. (3) and amplitude tapering coefficients given in Eq. (7), for vertical and horizontal polarization vectors \mathbf{p} separately. The exponent in Eq. (7) was $p=8$. Through simulations it has been found that choosing larger exponent does not further suppress the sidelobes. Figures 4 and 5 show examples of the directional responses in both the one and two signal cases for the beamforming analysis. Received power contours are shown with 1 dB interval.

Respectively, a grid of synthesized beams was used in the directional analysis, as described in the previous section. Figs. 6 and 7 present the same measurements as Figs. 4 and 5, but analyzed with the beam synthesis method.

Based on the responses presented in Figures 4–7, the directional properties of the spherical array for both the beamforming method and beam synthesis method are presented in Table 1.

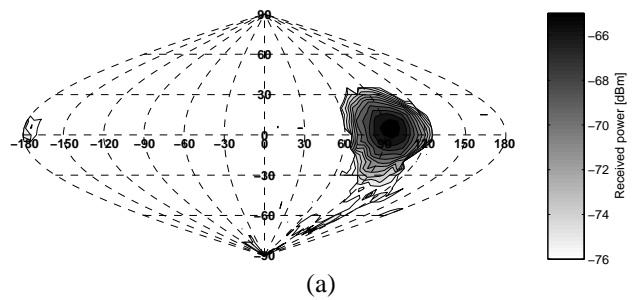


(a)

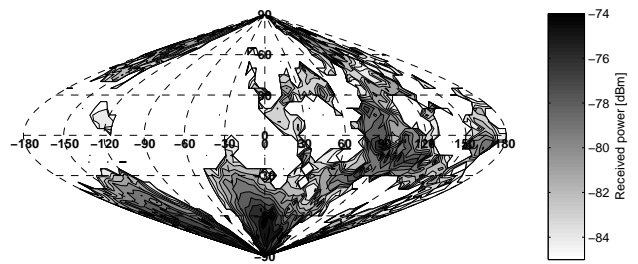


(b)

Figure 4. Directional response of the spherical array calculated with *beamforming* in the case of *one vertically polarized signal source* in direction $(+99^\circ, 0^\circ)$. (a) vertical polarization. (b) horizontal polarization.

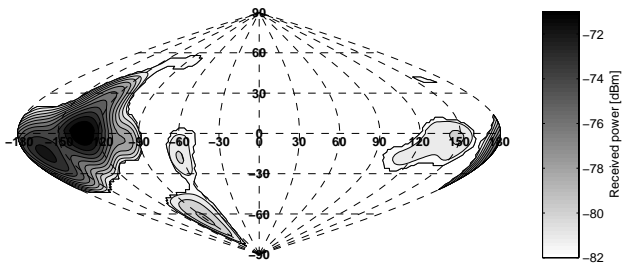


(a)

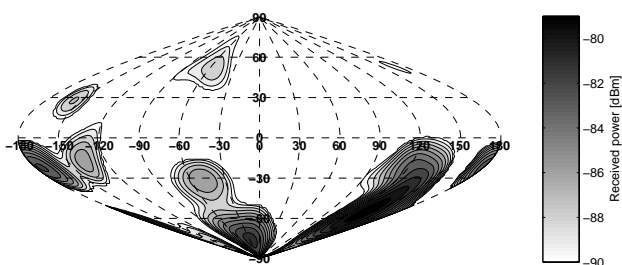


(b)

Figure 6. Directional response of the spherical array calculated with *beam synthesis* in the case of *one vertically polarized signal source* in direction $(+99^\circ, 0^\circ)$. (a) vertical polarization. (b) horizontal polarization.

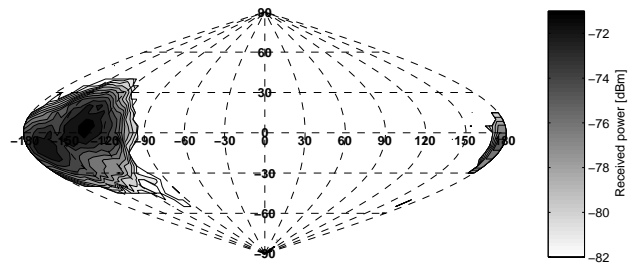


(a)

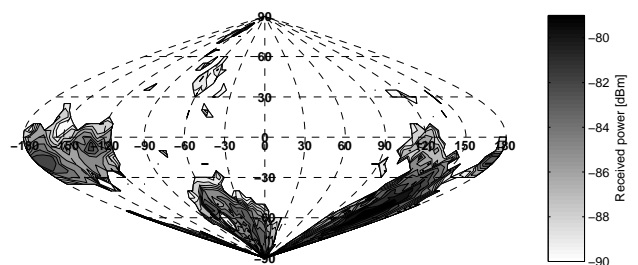


(b)

Figure 5. Directional array response calculated with *beamforming* in the case of *two signal sources* in directions $(-128^\circ, 0^\circ)$ and $(-159^\circ, -12^\circ)$. (a) vertical polarization. (b) horizontal polarization.



(a)



(b)

Figure 7. Directional array response calculated with *beam synthesis* in the case of *two signal sources* in directions $(-128^\circ, 0^\circ)$ and $(-159^\circ, -12^\circ)$. (a) vertical polarization. (b) horizontal polarization.

Table 1. Directional properties of the spherical array.

| | Beamforming | Beam synthesis |
|-----------------|-----------------|-----------------|
| Δ_{3dB} | $\sim 40^\circ$ | $\sim 40^\circ$ |
| SLL (1 signal) | -11 dB | -12 dB |
| SLL (2 signals) | -10 dB | -12 dB |
| XPD (1 signal) | 12 dB | 9 dB |
| XPD (2 signals) | 8 dB | 8 dB |

The uncertainty in the direction of arrival of the signal depends on the used angular grid in the calculations. Thus the uncertainty is 2° in the beamforming case and 5° in the beam synthesis case. The direction error caused by the sparse grid in the latter case can be seen in Figs. 6 and 7 as elevation offset from the horizontal plane.

The 3-dB beamwidth is said to be approximately 40° , since the two sources with angular separation of app. 40° in Figures 5 and 7 can be separated at -3 dB level.

It can be seen that the beam synthesis method produces slightly lower sidelobe level than the beamforming method. There is no considerable difference in the cross polarization levels.

The nonideal measurement of the phase of the element pattern has an effect to the performance of the beam synthesis. The element pattern was measured when attached to the array, and thus the accurate positioning of the element was difficult. The approximate error margin in the phase measurement is $\pm 10^\circ$.

In addition, the manufacturing tolerances of the elements and the array have an effect to the accuracy of the results. The manufacturing tolerances are 0.5 mm for the element and 1 mm for the array (element positions).

It has to be remembered though, that the sidelobes limit the directional dynamics of the measurement only in the case of multipaths with delay difference smaller than the delay resolution of the measurement (33 ns with 30 MHz code). Therefore, in most cases the dynamic range of the measurement is determined by the dynamic range of the used spreading code, and typically of the order of 30 dB.

5. Conclusions

This paper presents a method for directional 3D real-time measurements of the wideband mobile radio channel. The measurement method enables the separation of multipaths with the same excess delay and Doppler shift as long as their angular separation is not less than 40° , and path loss difference less than 11 dB. The polarization vector of the signal can also be measured with 9 dB dynamic range. The achieved delay resolution is 33 ns, which corresponds to path length of 10 m. The maximum mobile speed for $\pm 2\%$ phase accuracy is 10 m/s.

The directional and polarization accuracy of the measured radio channel were evaluated with two methods: beamforming by simple phasing of the elements, and numeric beam synthesis. The differences between the methods were found to be small. The beam synthesis method produces slightly lower sidelobe level, but is much more computationally complex, since the beams have to be synthesized separately for each angle in the chosen grid. The computational complexity required by the beamforming method is considerably lower.

The channel statistics that can be measured with the presented system can be used for evaluation of antennas for mobile handsets, as well as for developing polarization and radiation pattern diversity antennas for handsets.

Acknowledgments

The author wishes to thank Jani Ollikainen and Veli Voipio for helping in the design of the antenna element. Nokia foundation, Wihuri foundation, and Tekniikan edistämissäätiö are gratefully acknowledged for financial support.

References

- [1] K. Kalliola and P. Vainikainen, "Dynamic Wideband Measurement of Mobile Radio Channel with Adaptive Antennas", *Proceedings of 48th IEEE Annual Vehicular Technology Conference*, Ottawa, Ontario, Canada, May 18-21, 1998, pp. 21-25.
- [2] K.I. Pedersen, P.E. Mogensen, and B.H. Fleury, "Spatial Channel Characteristics in Outdoor Environments and their Impact on BS Antenna System Performance", *Proceedings of 48th IEEE Annual Vehicular Technology Conference*, Ottawa, Ontario, Canada, May 18-21, 1998, pp. 719-723.
- [3] K. Kalliola and P. Vainikainen, "Characterization System for Radio Channel of Adaptive Array Antennas", *Proceedings of 8th IEEE International Symposium on Personal, Indoor and Mobile Radio Communications*, Helsinki, Finland, September 1-4 1997, pp. 95-99.
- [4] J.R. Edmundson, "The Distribution of Point Charges on the Surface of a Sphere", *Acta Crystallographica*, A48, 1992, pp. 60-69.
- [5] L.I. Vaskelainen, "Iterative Least-Squares Synthesis Methods for Conformal Array Antennas with Optimized Polarization and Frequency Properties", *IEEE Transactions on Antennas and Propagation*, Vol. AP-45, July 1997, pp. 1179-1185.